736 *Journal of Electrical Engineering & Technology Vol. 7, No. 5, pp. 736~744, 2012*
http://dx.doi.org/10.5370/JEET.2012.7.5.736

Battery Charging System for PHEV and EV using Single Phase AC/DC PWM Buck Converter

Jung-Hyo Lee*, Doo-Yong Jung*, Sang-HoonPark, Taek-Kie Lee***, Young-Ryul Kim§ and Chung-Yuen Won†**

Abstract – In this paper, a battery charging system for Plug-in Hybrid Electric Vehicle (PHEV) and Electric Vehicle (EV), and operation algorithm of charging system are introduced. Also, the proposed charging system uses commercial electricity in order to charge the battery of parked PHEV and 48*V* battery charging system with power factor controllable single phase converter for PHEV is investigated in this paper. This research verifies the power factor control of input and the converter output controlled by the charge control algorithm through simulation and experiment.

Keywords: Plug-in hybrid electric vehicle, Electric vehicle, Battery charge, AC-DC PWM buck converter, CC-CV

1. Introduction

There has been active research to develop environmentally friendly products due to the recent increase in the oil prices and the reinforcement of strict environmental regulations worldwide. In particular, in order to develop environmentally friendly vehicles, there is active research in the automotive industry, which utilizes an immense amount of oil resources, on the drive system using electric motors and power-conversion systems that may potentially replace the conventional internal combustion engine [1, 2]. PHEV(Plug-in Hybrid Electric Vehicle), NEV(Neighborhood Electric Vehicle) and the general EV(Electric Vehicle) are examples of the new ecological vehicles. Such vehicles use electricity as its auxiliary and main power source, and battery is used as the energy source to drive their electric motors.

The batteries installed in electric vehicle systems can becharged through an external power distribution network through a plug [1, 2]. However, the battery is not charged by a simple connection through the plug; the incoming AC power from the external power distribution network must be converted into DC power in order to charge the battery.

Also, the power supply must be controlled in accordance with the proper specifications in order to charge the battery safely. Therefore, a power electronic battery charging system and its control system are needed to charge electric vehicle batteries.

† Corresponding Author: Dept. of Electrical Engineering, Sungkyunkwan Univerity, Korea. (woncy@skku.edu)
* Dept. of Electrical Engineering, Sungkyunkwan Univerity, Korea. (daumin@naver.com)
** Div. of Energy Component, LG Electronics. (shpark@lge.co.kr)
*** Dept. of Electrical Engineering, Hankyoung National Univerity, Korea. (tklee@hknu.ac.kr)
§ Dept. of Electrical Engineering, Anyang Univerity, Korea. (yrkim@anyang.ac.kr)
Received : February 20, 2012; Accepted : April 17, 2012

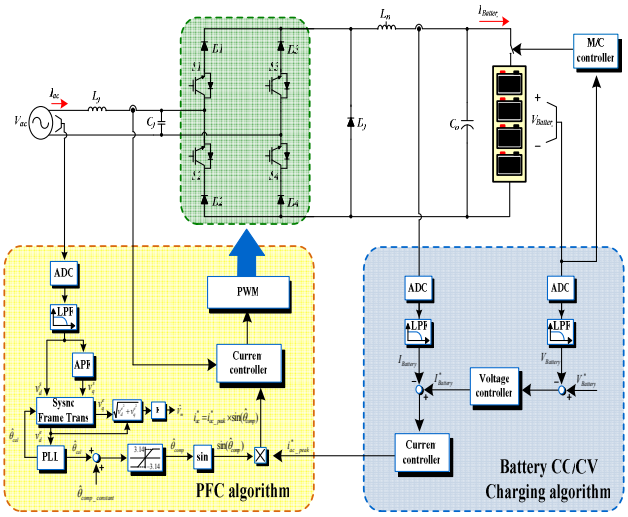

Fig. 1. Overall system and control block diagram of battery charger

The battery is used to the main energy source of electric vehicle. This paper is researched about the power conversion equipment for battery charging and control algorithm. The battery charging system was designed as a 48[V]/100[Ah] (Charging current=20[A]/1[Hour], charging voltage=50.7[V]) system by providing serial connection of 4lead-acid batteries (12[V]/100[Ah]).

The designed charging system was controlled to charge the batteries a low-voltage($V_{battery}$=50.7[*V*])of the batteries from a high-voltage input(V_{rms}=220[*V*]/60[*Hz*]) by using the single-phase AC/DC PWM Buck Converter Topology [3-7], serial constantcurrent/constantvoltage charging control [8] and PFC algorithms [9, 10].

In this research, battery charging system is composed of converter, controller, gate driver and SMPS. The controlleris comprised of TI's TMS320F28335, a 32Bit

DSP that is capable of fixed decimal position calculations, and EPM7128SQL100-10, ALTERA's EPLD, for fault signals and I/O expansion. The converter in this research is designed using the single-phase AC/DC PWM Buck Converter topologythat is similar to structure of the full-bridge converter.

The performance of the system in the researchis verified through simulation by using PSIM 6.0 and experiment by the 1.2[kW] battery charging system.

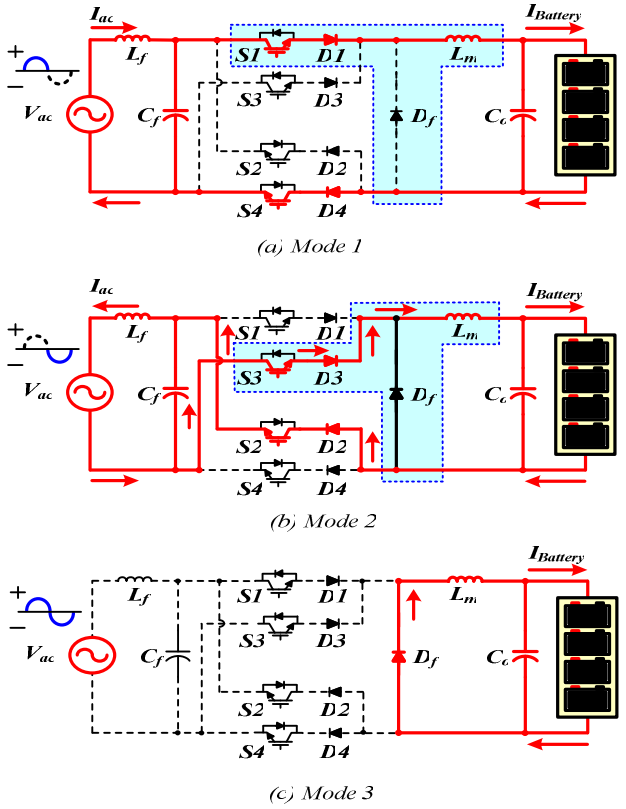

Fig. 2. Operational mode of battery charger using AC/DC PWM buck converter

2. Descriptions of proposed charging system

Fig. 1 shows the overall system block diagram.These the battery charging system was designed by applying a single-phase AC/DC PWM Buck converter [3, 5]. The topology applied in this research consists of IGBT, a power semiconductor switching device, and a switch block with diodes connected in series, which is similar to a full-bridge converter. However, as for the applied converter, the collector and the emitter of the IGBT are in the reverse direction unlike the general full-bridge converter, and the emitter of the switch is serially connected with the diodes.

Such structure induces operation in the Buck mode [3-5], which is equivalent to that of the operation seen in Fig. 2. The battery charging algorithm applied in this research consists of two parts as shown in Fig. 1.

In Fig. 1, the first control block is the control algorithm for the input power factor control. In this control block, APF generates a virtual two-phase d-axis and q-axis stationary reference frame signal from a single-phase power supply. The generated stationary reference frame signal is then converted into a synchronous reference frame, and the phase angle of the single-phase input voltage is estimated through the PLL control.

The second control block is the control algorithm for constant-current and constant-voltage control. The battery is charged through the algorithm as safe. Also, the output of current controller can be the peak reference of the input current and it is applied for PFC by multiplying estimated phase angle. Fig. 2 shows the circuit diagram, which is an equivalent circuit of the single-phase AC/DC PWM Buck Converter shown in Fig. 1, in order to facilitate the analysis of the operating mode [6, 7].

Mode 1 (Fig. 2(a)) –For half a positivecycle of input voltage, Mode 1 is operated.When switch block-1(*S1*and *D1)* and switch block-4(*S4*and *D4)* are turned on, the battery of output terminal is charged.

Mode 2 (Fig. 2(b)) –For half a negative cycle of input voltage, mode 2 is operated. When switch block-2(*S2*and *D2)* andswitch block-3(*S3*and *D3)* are turned on, the battery of output terminal is charged.

Mode 3 (Fig. 2(c)) –When all of switch block are turned off, mode 3 is operated in freewheeling.The stored energy of main inductor (L_m) is transferred to load through diode (D_f), and capacitor (C_o).

3. Design Procedure

In Fig. 1, input L-C filter of battery charging systemto input terminal is designed with following specifications.

3.1 Inductor design of input L-C filter

The input impedance was decided by rms of the input voltage($V_{ac,rms}$) and the rated capacity of the battery charging system. The impedance can be calculated by (1).

$$Z_{in}=\frac{(V_{ac\_rms})^2}{P_{rate}}=\frac{220^2[V^2]}{1200[W]}\simeq 40.334[\Omega] \quad (1)$$

Designed impedance of filter inductor is smaller than whole impedance. In this research, the impedance of inductor (Z_{Lf}) is designed to 5% of whole impedance by (2). Therefore, inductance(L_f) of filter inductor is given by (3).

$$Z_{L_f}=40.334\times 0.05=2.0167[\Omega] \quad (2)$$

$$L_f = \frac{Z_{Lf}}{2\pi f_{grid}} = \frac{2.0167}{2\times 3.141592\times 60} \simeq 5.35[mH] \quad (3)$$

3.2 Capacitor design of input L-C filter

The capacitor (C_f) of input L-C filter was calculated by inductance of input inductorand resonant frequency (f_r) of L-C filter. In this case the maximum resonant frequency ($f_{r,max}$) is equal to half a switching frequency by (4). The resonant frequency (f_r) is given by (2).

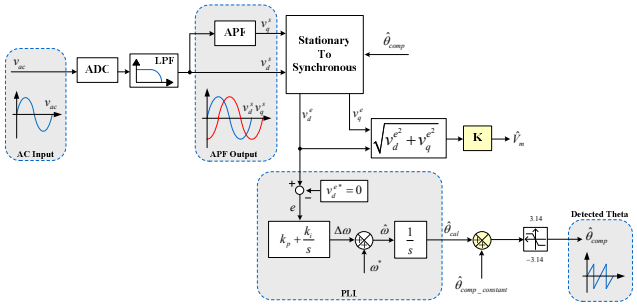

Fig. 3. Detection control block diagram of phase angle of input grid voltage

$$f_{r\_\max} = 0.5\times f_{sw} \quad (4)$$

$$f_r = 0.8\times f_{r\_\max} = 0.8\times 0.5\times 10000 = 4[kHz] \quad (5)$$

Therefore, (6) must be satisfied. The capacitor(C_f) of input L-C filter is given by (7).

$$f_r = \frac{1}{2\pi\sqrt{L_f C_f}} \quad (6)$$

$$C_f = \frac{1}{(2\pi f_r)^2 \times L_f} = \frac{1}{(2\times 3.141592\times 4000)^2 \times 0.00535} = 0.295[\mu F] \quad (7)$$

3.3 Design of output filter inductor

Inductor (L_m) of output filter is expressed by (8). Therefore,inductor (L_m) in output filter is given by (9).

$$L_m = \frac{t_{on}}{\Delta i_L}\times(V_{ac\_avg} - V_{battery}) = \frac{G_v T_{sw}}{\Delta i_L}\times(V_{ac\_avg} - V_{battery}) \quad (8)$$

$$L_m = \frac{0.41223\times 100[\mu s]}{1[A]}\times(220[V] - 50.7[V]) = 6.979[mH] \quad (9)$$

4. System control algorithms

Fig. 3 shows the control block diagram of PFC algorithm in input terminal [11].

The input voltage obtained by ADC flows through LPF and $\hat{\theta}_{\text{cal}}$ can be calculate by synchronous transformation frame and single phase PLL. PFC is achieved through input current controller using detected $\hat{\theta}_{\text{comp}}$.The control algorithm for constant current and constant voltage is shown in Fig. 6. Peak reference value of input current $i^*_{ac\text{-}peak}$ is equal to value of the charging controller. Input current reference i^*_{ac} is generated by multiplying peak reference value of input current and unit sine wave.

4.1 All pass filter

APF(AllPass Filter) has not magnitudeattenuation characteristics, which affects the design for PLL.In this paper, PFC controller need a signal which is the stationary reference frame with virtual 2 phase type for detection phase angle of single grid voltage. v_q^s is obtained through APF with input voltage v_{ac} and it is delayed 90° than input voltage. The transfer function of analog type APF is given by (10).

$$\begin{aligned} H(s) = H(j\omega) &= \frac{-1+j\omega CR}{1+j\omega CR} \\ &= \frac{\sqrt{(-1)^2+(\omega CR)^2}\angle\tan^{-1}\left(\frac{-\omega CR}{1}\right)}{\sqrt{(1)^2+(\omega CR)^2}\angle\tan^{-1}\left(\frac{\omega CR}{1}\right)} \\ &= 1\angle\left[\tan^{-1}(\omega CR) - \tan^{-1}(-\omega CR)\right] \\ &= 1\angle 2\tan^{-1}(\omega CR) \quad \because \omega_c = \frac{1}{CR} \end{aligned} \quad (10)$$

Digital filter which is based on DSP is expressed as follows (11)-(13).

$$\begin{aligned} H(s) &= \frac{-1+sCR}{1+sCR} = \frac{-1+\frac{s}{\omega_c}}{1+\frac{s}{\omega_c}} = \frac{s-\omega_c}{s+\omega_c} \quad \leftarrow \quad \omega_c = \frac{1}{CR} \\ &= \frac{-\omega_c + \left(\frac{2}{T}\times\frac{1-Z^{-1}}{1+Z^{-1}}\right)}{\omega_c + \left(\frac{2}{T}\times\frac{1-Z^{-1}}{1+Z^{-1}}\right)} = \frac{-(\omega_c T-2) - (\omega_c T+2)\cdot Z^{-1}}{(\omega_c T+2) + (\omega_c T-2)\cdot Z^{-1}} \\ &\because \begin{cases} A = \omega_c T + 2 \\ B = \omega_c T - 2 \end{cases} \end{aligned} \quad (11)$$

$$H(z) = \frac{B+AZ^{-1}}{A+BZ^{-1}} = \frac{y[n]}{x[n]} \quad (12)$$

$$\rightarrow \quad \left(A+BZ^{-1}\right)\cdot y[n] = \left(B+AZ^{-1}\right)\cdot x[n]$$

$$A\cdot y[n]+B\cdot y[n-T]=B\cdot x[n]+A\cdot x[n-T]$$

$$\therefore y[n]=\left(\frac{B}{A}\cdot x[n]+x[n-1]\right)-\left(\frac{B}{A}\cdot y[n-T]\right) \quad (13)$$

4.2 Synchronous transformation frame and PLL

The output of the virtual two-phase stationary reference frame is used as the synchronous reference frame, and then outputs the q-axis component, which indicates the magnitude of the input voltage, and the d-axis component, which indicates the error of the phase angle are produced [12].

$$v_d^e = v_d^s \cos\hat{\theta} + v_q^s \sin\hat{\theta} \quad (14)$$

$$v_q^e = -v_d^s \sin\hat{\theta} + v_q^s \cos\hat{\theta} \quad (15)$$

The d-axis component, which indicates phase angle error,is used as the input for the PLL of the PI-controller after being compared with the d-axis voltage reference. The output from the PI-controller is added to the reference value of the phase angle frequency of grid, which is a feed-forward component, to be used to estimate the phase angle frequency. The estimated phase angle frequency is then converted into a phase angle of the input voltage through an integrator.

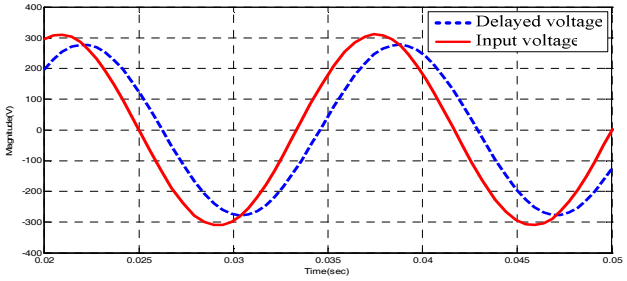

(a) The waveforms of input voltage and output voltage through the 1st LPF.

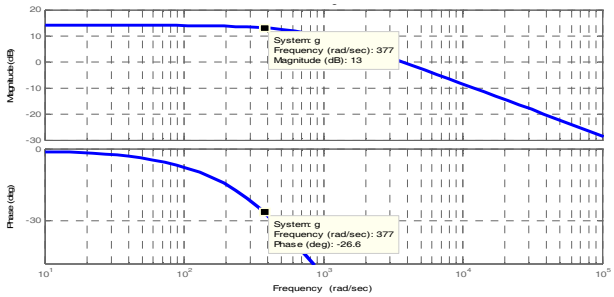

(b) The bode diagram of output voltagethrough the 1st LPF.

Fig. 4. Output characteristic and bode diagram of the 1st LPF

4.3 Compensation of detected theta

The digital Low-Pass-Filter(LPF) removes the noise of the grid voltage sensed through the Analog-to-Digital Converter(ADC). However, the signal through the low-pass filter can occur original signal magnitude attenuation and phase delay according to the cut-off frequency range.

Therefore, in order to accurately estimate the phase angle of the grid voltage that is used to control the input power factor, the phase delay must be compensated as much as it is delayed. The following Fig. 4 shows the bodeplot that shows the magnitude attenuation due to the LPF, the characteristics of the filter and the voltage waveform that indicates a phase delay.

Cut-offfrequency of LPF is 120 [*Hz*] which is 2 times the frequency of input voltage. Magnitude attenuation and delay phase of filter are calculated as follows.

$$|G(j\omega)| = \left|\frac{1}{\sqrt{j\frac{\omega_{input}}{\omega_{cutoff}}+1}}\right| = \frac{1}{\sqrt{\left(\frac{\omega_{input}}{\omega_{cutoff}}\right)^2+1}} = \frac{1}{\sqrt{\left(\frac{2\pi\times 60}{2\pi\times 120}\right)^2+1}} \simeq 0.894[dB] \quad (16)$$

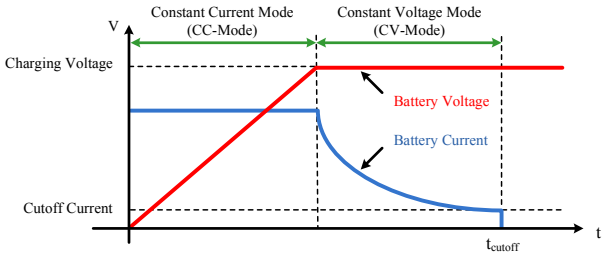

Fig. 5. The characteristic curve of battery voltage and current at CC/CV mode

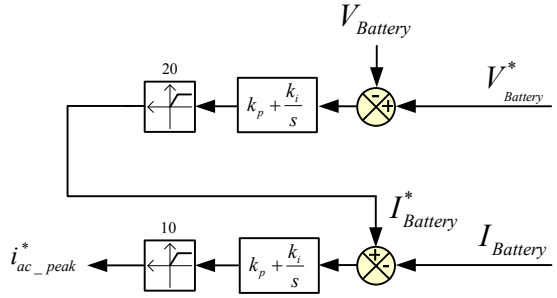

Fig. 6. Control block diagram of series type CC/CV mode

In Fig. 4, PFC is achieved as well through compensator by (16) and (17). Also, magnitude attenuation and phase delay are compensated.

$$\angle G(j\omega)=\angle\left(\frac{1}{j\frac{\omega_{input}}{\omega_{cutoff}}+1}\right)=-\tan^{-1}\left(\frac{\omega_{input}}{\omega_{cutoff}}\right) \quad (17)$$
$$=-\tan^{-1}(0.5)\simeq-26.56[\text{deg}]$$

4.4 Battery CC-CV charging control algorithm

Fig. 5 shows the characteristic curve of the battery charging method that uses constant current/constant voltage algorithms. In the initial period, the battery charging system is operated in a constant current mode, and the voltage of the battery gradually increases as the constant current set by the charging current value is applied to the battery.

Then, when the voltage of the battery rises to the designed charging value, it will change to the constant voltage mode. At this point, the current applied to the battery will be gradually reduced.

When the current is slowly reduced at the constant voltage mode and the current of the battery reaches the point of the cut-off current, the battery is determined to be fully charged. At this point, all the PWM of the switching device are disabled, and after amount of the time (when the energy stored in the output inductor is fully discharged), the M.C is blocked and the connection between the charging unit and the battery isseparated .

4.5 PFC algorithm

Fig. 7 shows the control block diagram of PFC algorithm in input terminal. Unit sine wave is obtained by compensated theta and sine function. Input current reference i^*_{ac} is generated by multiplying peak reference value of input current and unit sine wave.

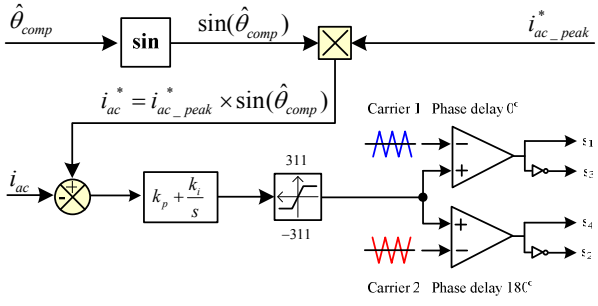

Fig. 7. Control block diagram of power factor correction

5. Simulation Results

Fig. 8 is the program flowchart that shows the power factor control and battery charging algorithm applied in this research. At every interrupted interval (100[us]), the input voltage and current, and the voltage and current of the battery are sensed by triggering the ADC. The controller is composed of a power factor controller that is executed every 100[us] and the constant current/constant voltage controller that is operated every 1[ms].

The power factor controller is performed every 100[us] to detect the phase angle of the input grid voltage, and the constant current/constant voltage controller is implemented every 1[ms] to generate the reference (maximum value) of the input current. The value generated by multiplying these two control values is used as the reference of the current controller.

Table 1 is specifications of the battery charging systemto simulation and experiment. Table 2 is specifications of the battery and the battery bank.

Fig. 9 shows the simulation waveform that indicates the input voltage and current, the phase angle of the input voltage and the input voltage frequency. Through this waveform that resulted from a simulation, we can confirm that the phase angle of the input voltage can be estimated properly by using the virtual two-phase method, synchronous transformation frame and PLL. Also, we can con-firm that the input current is well-controlled as much as the input voltage through the PFC. Fig. 10 is the waveform that represents the result of the simulation, which shows the input voltage and current, and the charging current and voltage of the battery.

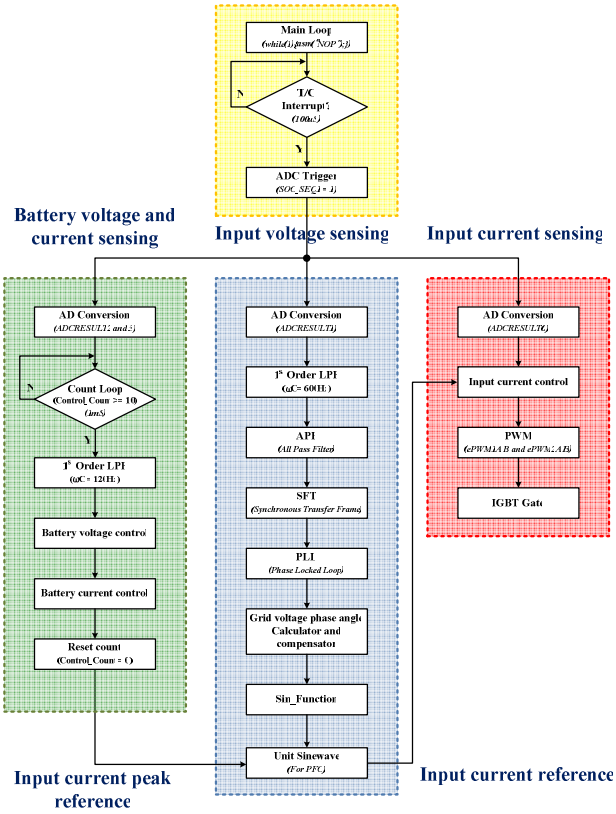

Fig. 8. Program flow chart of developed battery charger

Table 1. Parameters of battery charger

Input Voltage	V_{ac}	$220V_{rms}$
Charging Voltage	$V_{Battery}$	$50.7V$
ChargingCurrent	$I_{Battery}$	$20A$
Switching Frequency	f_s	$10kHz$
Input Filter Inductor	L_f	$5.5mH$
Input Filter Capacitor	C_f	$0.32\mu F$
OutputFilter Inductor	L_m	$7mH$
Output Capacitor	C_o	$7100\mu F$

This waveform representing the results of the simulation confirms that when the battery is charged during the initial period, soft-start is performed for a designated period of time and the voltage of the battery is gradually charged as the constant current mode is in operation. Also, when the voltage of the battery reaches the set charging voltage, the current that flows into the battery begins to decrease as it switches to the constant voltage mode. When the current inflow to the battery starts to decrease and reaches the cutoff current point, the battery is determined to be fully charged. Then, at this point, all the PWM signals are disabled, and the M.C is blocked to prevent the battery from becoming overcharged.

Table 2. Specifications of battery, battery bank and charging conditions

Battery Model.	DELKOR Hi-Ca 100 (Lead-Acid)	
Nominal Voltage.	$12V$	
Typical Capacity.	$100Ah$	
Charge Condition.	Max. Current.	$20A$
	Max. Voltage.	$14.5 \sim 14.8V$
Discharge Condition.	Continuous Current.	$80A$
	Max. Current.	$200A$
	Cut-Off Voltage.	$11.4V$
Life Cycle.	> 2500 Cycle @ 80% DoD	
Battery Bank Construction (12[V]×4EA=48[V]).	Charging Voltage.	$50.7V$
	Charging Current.	$20A$
	Cut-Off Current.	$2A$
	Max.Allowable Voltage.	$53.3V$

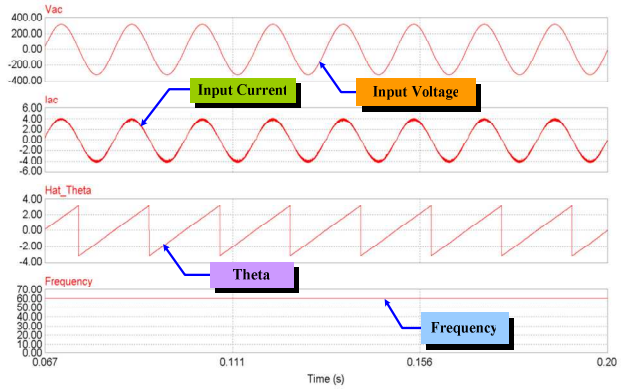

Fig. 9. Simulation results of the input voltage, input current, frequency and phase angle of input voltage

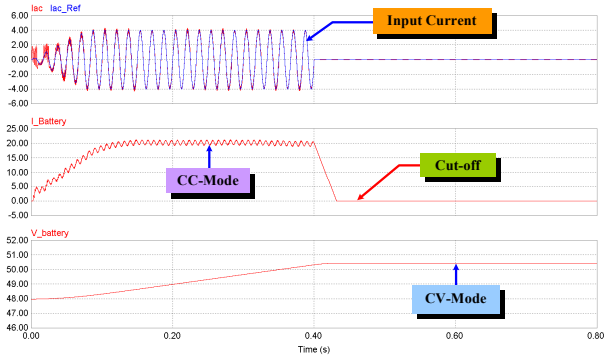

Fig. 10. Simulation results of the input current, battery current and battery voltage

6. Experiment Result

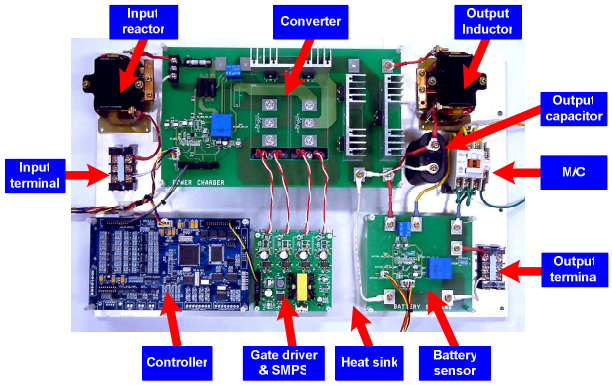

Fig. 11. System setup of battery charger

Fig. 11 shows the experiment setup of the 1.2[kW] battery charging system that was designed in this research. The experiment setup is composed of a controller, power conversion system, input and output filters, sensors, circuit breakers, and the 4-channel gate drive with the design of the Flyback SMPS.

In a battery charging system that is composed of such parts, the single-phase grid power is supplied to the power conversion system from the input terminal through the input filter, and the converted energy charges the battery through the output filter as well as the M.C for interruption purposes (M.C turn-on state).

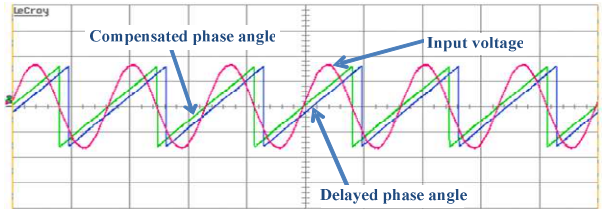

Fig. 12. Experimental results of input voltage and delayed and compensated phase angle.(Input voltage; Y-axis=200[V/div.], Delayed and compensated phase angle; Y-axis=2[V/div.], X-axis=10[ms/div.])

Fig. 12 is the experimental waveform that shows the input grid voltage, the estimated phase angle of the delayed grid voltage due to a low-pass filter, and the phase angle that was compensated for a phase delay. This waveform confirms that the phase of the delayed estimated phase angle was delayed compared to the input grid voltage waveform. Also, we can confirm that the phase angle that was compensated for the phase delay was controlled in precise synchronization with the input grid voltage control.

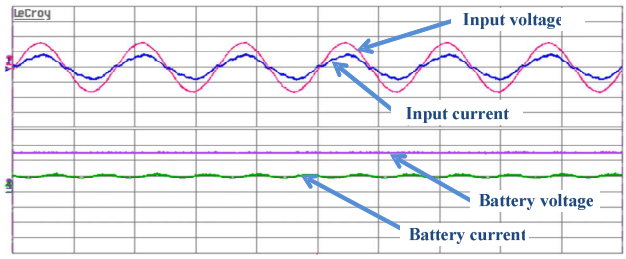

Fig. 13. Experimental results of input voltage, input current and battery voltage. (Input voltage; Y-axis=200[V/div.], Input current; Y-axis=4[A/div.], Battery voltage; Y-axis=20[V/div.], Battery current; Y-axis=20[A/div.], X-axis=10[ms/div.])

Fig. 13 shows the waveform from the results of the experiment that measured the input grid voltage and current, and the voltage and current of the battery. This experimental waveform confirms that the input power factor control operates well. Also, we confirmed that the battery was being charged gradually with a constant charging current in the constant current mode.

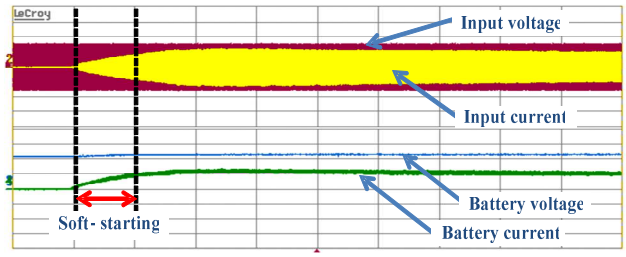

Fig. 14. Experimental results of input voltage, Input current, battery voltage and current in initial constant current mode. (Input voltage; Y-axis = 200[V/div.], Input current; Y-axis = 4[A/div], Battery voltage; Y-axis = 20[V/div.], Battery current; Y-axis = 20[A/div.], X-axis = 2[s/div.], Battery initial voltage = 44[V])

Fig. 14 shows the experimental waveform that indicates the constant current mode. This is a waveform that measures the mode, in which the voltage of the battery is slowly charged in a stable manner in the constant current mode during the initial stage when the battery is completely discharged at the initial voltage of 44[V]. As it is seen in this experimental waveform, the voltage of the battery gradually increases as a specific magnitude of the charging voltage is applied to the battery. At this time, the magnitude of the input current will also be specific because it is in the constant current mode.

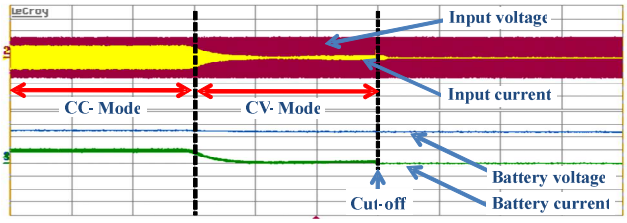

Fig. 15. Experimental results of input voltage, input current, battery voltage and current in constant voltage mode. (Input voltage; Y-axis = 200[V/div.], Input current; Y-axis = 4[A/div], Battery voltage; Y-axis = 20[V/div.], Battery current; Y-axis = 10[A/div.], X-axis = 2[s/div.], Battery chargingvoltage = 50.7[V])

Fig. 15 shows the experimental waveform that indicates constant voltage and the interrupted mode. This experimental waveform confirms that it switches from the constant current mode to the constant voltage mode when the voltage of the battery reaches 50.7[V], the set charging voltage. When it starts to operate in the constant voltage mode, the current that is applied to the battery is reduced, and it will flow with the magnitude of the cutoff current. However, the voltage of the battery is maintained at a constant charging voltage. When it is determined that the battery is fully charged after the cutoff current flows into the battery for a designated period of time, the connection between the charging device and the battery is blocked and the inflow of the current into the battery is stopped to prevent overvoltage.

7. Conclusion

This research paper proposed a charging system for electric vehicle batteries, which utilizes the input from an external single-phase grid power, and the algorithms to control the system. The designed battery charging system applies the single-phase AC/DC PWM Buck Converter Topology, which charges batteries with a low voltage (50.7[V]) from an input of a high voltage(220[V_{rms}]), with a power factor control.

Furthermore, by applying the power factor control algorithms using serially connected constant current/ constant voltage charging algorithm, APF, STF, and PLL, the performance and feasibility of the 1.2[kW] battery charging system designed in the research were verified with the simulation and experimental results.

Acknowledgements

This work was supported by the National Research Foundation of Korea(NRF) grant funded by the Korea government(MEST) (No.2012-0005371)

References

[1] Ali Emadi, Young Joo Lee,Kaushik Rajashekara, "Power electronics and motor drives in electric, hybrid electric, and plug-in hybrid electric vehicles," *IEEE Transactions on Industrial Electronics*, Vol. 55 , No.6, pp.2237-2245, Jun 2008.

[2] Young-Joo Lee, Alireza Khaligh, Ali Emadi, "Advanced Integrated Bidirectional AC/DC and DC/DC Converter for Plug-In Hybrid Electric Vehicles," *IEEE Transactions on vehicular technology*, Vol. 58, No. 8, pp.3970-3980, Oct 2009.

[3] Ramesh Oruganti, Moorthi Palaniapan, "Inductor voltage controlled variable power factor buck-type AC-DC converter," 27th Annual IEEE Power Electronics Specialists Conference, Vol. 1, pp.230-237, Jun 1996.

[4] Ramesh Oruganti, Moorthi Palaniapan, "Enhanced control design of single phase AC-DC converter using power balance calculator," 4th International Power Electronics and Motion Control Conference, Vol. 3, pp. 1101-1104, Aug 2004.

[5] Ramesh Srinivasan, Moorthi Palaniapan, Ramesh Oruganti, "A Single Phase Two-Switch Buck Type AC-DC Converter Topology with Inductor Voltage Control," 28th Annual IEEE Power Electronics Specialists Conference, Vol. 1, pp. 556-563, Jun 1997.

[6] Ramesh Oruganti, Moorthi Palaniapan, "Inductor Voltage Control of Buck-Type Single-Phase AC–DC Converter," *IEEE Transactions on power electronics*, Vol. 15, No. 2, pp.411-416, May 2000.

[7] Bhim Singh, Brij N. Singh, Ambrish Chandra, Kamal Al-Haddad, Ashish Pandey, and Dwarka P. Kothari, "A Review of Single-Phase Improved Power Quality AC-DC Converters," *IEEE Transactions on Industrial Electronics*, Vol. 50, No.8, pp.962-981, Oct 2003.

[8] Chanakya B. Bhatt, Vinod P. Patel and Nimit K. Sheth, "High Voltage Battery Charger,"International Conference on Electrical Machines and Systems 2007, pp.1772-1777, Oct 2007.

[9] Michael G. Egan, Dara L. O'Sullivan, John G. Hayes, Michael J. Willers,Christopher P. Henze, "Power-Factor-Corrected Single-Stage Inductive Charger for Electric Vehicle Batteries," *IEEE Transactions on Industrial Electronics*, Vol. 54, No. 2, pp.1217-1226, Apr 2007.

[10] Ramesh Oruganti, Ramesh Srinivasan, "Single phase power factor correction - A review," *Sadhana*, Vol. 22, Part 6, pp. 753-780, Dec 1997.

[11] Chen Xiyon Yan Bin,Gao Yu, "The Engineering design and optimization of inverter output RLC filter in AC motor drive system," IECON02, Vol.1, pp.175-180, 2002.

[12] Antonio Cataliotti, Valentina Cosentino, Salvatore Nuccio, "A Phase-Locked Loop for the Synchronization of Power Quality Instruments in the Presence of Stationary and Transient Disturbances," *IEEE Transactions on Instrumentation and Measurement,* Vol. 56, No. 6, pp. 2232-2239, Dec 2007.

[13] Keun-Young Kim, Sang-Hoon Park, Seung-Kyung Lee, Taeck-Kie Lee, Chung-Yuen Won, "Battery charging system for PHEV and EV using single phase AC/DC PWM buck converter," VPPC2010,Sep 2010.

Jung-Hyo Lee He received the B.S degree in electrical engineering from Konkuk University,Seoul, Korea, in 2006, and the M.S degree in Electrical Engineering from Sungkyunkwan University, Suwon, Korea, in 2008. He is currently working toward Ph.D degree in Sungkyunkwan University. His research interests include robust control of power electronic devices and advanced motor drive control.

Doo-Yong Jung He received the B.S degree in electrical engineering from Anyang University Anyang, Korea,in 2007, and the M.S degree in photovoltaic system engineering from Sungkyunkwan University,Suwon, Korea,in 2009, where he is currently working toward the Ph. D. degree in graduate school of photovoltaic system engineering His research interests include converters, inverters and its control for smart-grid applications

Sang-HoonPark He received the B.S degree in Konyang University,Nonsan, Korea, in 2005, and M.S and Ph.D degree in electrical engineering from Syngkyunkwan University Suwon, Korea, in 2007, 2011, respectively. From 1982 to 1987, Since 2011, He is a senior researcher of Energy Component (EC) Division in LG Electronics,Seoul, Korea. His research interests include power electronics, power converters, and electrical drives.

Taek-Kie Lee He received the B.S and M.S and Ph.D degree in electrical engineering from Hanyang University, Seoul, Korea, in 1987, 1989, 1993, respectively. From 1994 to 1996, From 1994 to 1996, he was with the Department of Electrical Engineering, Seonam University, Namwon, Korea. Since 1996, he has been with Hankyong National University, Ansung, Korea, where he is a Professor with the Department of Electrical, Electronic and Control Engineering. He was a Visiting Professor in the Energy Power Research Center, Sungkyunkwan University in 2010. His research interests include power electronics, power converters, and electrical drives.

Young-RyulKim He received the B.S and M.S and Ph.D degree in electrical engineering from Seoul National University, Seoul, Korea,in 1982, 1989, 1993, respectively. From 1982 to 1987, He was a researcher of Enterprise Technology Support Center (ETSC) in Korea Institute of Machinery and Materials. From 1993 to 1996, He was a senior researcher of Korea Aerospace Research Institute. Since 1996, he is currently a professor in electrical engineering Anyang University,Anyang, Korea.His research interests include power electronics, power converters, and electrical drives.

Chung-Yuen Won He received the B.S. degree in electrical engineering from Sungkyunkwan University, Suwon, Korea, in 1978 and the M.S. and Ph.D. degrees in electrical engineering from Seoul National University, Seoul, Korea, in 1980 and 1988, respectively. From 1990 to 1991, he was with the Department of Electrical Engineering, University of Tennessee, Knoxville, as a Visiting Professor. Since 1988, he has been a Faculty Member with Sungkyunkwan University, where he is currently a Professor in School of Information and Communication Engineering. He was the President of the Korean Institute of Power Electronics at 2010. His research interests include dc–dc converters for fuel cells, electromagnetics modeling and prediction for motor drives, and control systems for rail power delivery applications.